Accepted Preprint first posted on 27 January 2017 as Manuscript JOE-16-0451

Hormone deprivation alters mitochondrial function and lipid profile in the hippocampus

Sandra Zárate[1,2], Mariana Astiz[3†], Natalia Magnani[4††], Mercedes Imsen[1], Florencia Merino[1], Silvia Álvarez[4], Analía Reinés[5], Adriana Seilicovich[1,2]

[1]Instituto de Investigaciones Biomédicas (INBIOMED, UBA-CONICET)

[2]Departamento de Histología, Embriología, Biología Celular y Genética, Facultad de Medicina, Universidad de Buenos Aires, Buenos Aires, Argentina.

[3]Instituto de Investigaciones Bioquímicas de La Plata (INIBIOLP, UNLP-CONICET) and Cátedra de Bioquímica y Biología Molecular, Facultad de Medicina, Universidad Nacional de La Plata, La Plata, Argentina.

[†]Current address: University of Lübeck, Medical Department I, Lübeck, Germany.

[4]Instituto de Bioquímica y Medicina Molecular (IBIMOL, UBA-CONICET), Facultad de Farmacia y Bioquímica, Universidad de Buenos Aires, Buenos Aires, Argentina.

[††]Current address: Division of Pulmonary and Critical Care Medicine, Northwestern University Feinberg School of Medicine, Chicago, Illinois, USA.

[5]Instituto de Biología Celular y Neurociencias 'Prof. E. De Robertis' (IBCN, UBA-CONICET), Facultad de Medicina and Cátedra de Farmacología, Facultad de Farmacia y Bioquímica, Universidad de Buenos Aires, Buenos Aires, Argentina.

Corresponding author:

Sandra Zárate

Instituto de Investigaciones Biomédicas
Universidad de Buenos Aires-CONICET
Facultad de Medicina,
Paraguay 2155, piso 10
Buenos Aires (C1121ABG)
ARGENTINA
szarate@fmed.uba.ar
TEL/FAX + 54 11 5950 9612

Short title: Ovariectomy alters mitochondrial function & lipids

Keywords: mitochondria; ovariectomy; hippocampus; PUFAs; cardiolipin; aging

Text word count: 6064

Abstract

Mitochondrial dysfunction is a common hallmark in aging. In the female, reproductive senescence is characterized by loss of ovarian hormones, many of whose neuroprotective effects converge upon mitochondria. Mitochondria functional integrity is dependent on membrane fatty acid and phospholipid composition, parameters also affected during aging. The effect of long-term ovarian hormone deprivation upon mitochondrial function and its putative association with changes in mitochondrial membrane lipid profile in the hippocampus, an area primarily affected during aging and highly responsive to ovarian hormones, is unknown. To this aim, Wistar adult female rats were ovariectomized or sham-operated. Twelve weeks later, different parameters of mitochondrial function (O_2 uptake, ATP production, membrane potential and respiratory complex activities) as well as membrane phospholipid content and composition were evaluated in hippocampal mitochondria. Chronic ovariectomy reduced mitochondrial O_2 uptake and ATP production rates and induced membrane depolarization during active respiration without altering the activity of respiratory complexes. Mitochondrial membrane lipid profile showed no changes in cholesterol levels but higher levels of unsaturated fatty acids and a higher peroxidizability index in mitochondria from ovariectomized rats. Interestingly, ovariectomy also reduced cardiolipin content and altered cardiolipin fatty acid profile leading to a lower peroxidizability index. In conclusion, chronic ovarian hormone deprivation induces mitochondrial dysfunction and changes in the mitochondrial membrane lipid profile comparable to an aging phenotype. Our study provides insights into ovarian hormone loss-induced early lipidomic changes with bioenergetic deficits in the hippocampus that may contribute to the increased risk of Alzheimer's disease and other age-associated disorders observed in post-menopause.

Introduction

Mitochondria are key organelles for cellular bioenergetics and survival. They are the main source of ATP production through oxidative phosphorylation by the mitochondrial respiratory chain and also the primary sites for cellular reactive oxygen species (ROS) generation. As an organ with a high demand of energy and low antioxidant capacity, the brain is particularly vulnerable to mitochondria dysfunction and oxidative stress, interdependent mechanisms that play a central role in brain aging (Chakrabarti *et al.* 2011). Aging is an inevitable biological process characterized by a progressive decline in physiological functions and increased susceptibility to disease. It is now accepted that normal aging and several aging-related diseases, such as Alzheimer's and Parkinson's, are related to mitochondrial dysfunction (Chakrabarti *et al.* 2011, Johri & Beal 2012). Sex steroid hormones, especially estrogens, have been widely investigated in relation to brain aging. Multiple lines of evidence point for brain mitochondria as targets of steroid hormone action (Jones & Brewer 2009, Arnold *et al.* 2012). In fact, a link between sex-dependent susceptibility and mitochondrial dysfunction has been identified in normal aging as well as in neurodegenerative diseases both in preclinical animal studies and in women after menopause (Rasgon *et al.* 2005, Yao *et al.* 2010, Johri & Beal 2012). Collectively, data from animal studies indicate that the decline in whole brain mitochondrial function associated with reproductive senescence is due to loss of ovarian hormones (Yao *et al.* 2009, Yao *et al.* 2010, Yao *et al.* 2012). Unlike primates, the loss of reproductive cycles during aging in the rat does not occur concomitant with ovarian follicular atresia and its associated decline in estradiol levels. Rather, middle-aged acyclic rats are in a state of persistent estrus with chronically high estradiol levels and thus are not considered a good model for reproductive aging. Instead, ovariectomy has been widely used as a more appropriate model for reproductive aging in the rat (Morrison *et al.* 2006). Detrimental effects of ovarian hormone deprivation upon mitochondrial bioenergetics include reduced respiration and ATP

production rates, increased oxidative stress and decreased expression and/or activity of metabolic enzymes within this organelle (Shi *et al.* 2011, Irwin *et al.* 2011, Yao *et al.* 2012, Gaignard *et al.* 2015). The vast majority of animal studies about steroid hormone modulation of mitochondrial function have been performed in the whole brain, without the dissection of different brain areas that have dissimilar response to ovarian hormones. Indeed, brain mitochondrial dysfunction in aged animals is more evident in specific brain areas, among which the hippocampus emerges as an early target of both aging and ovarian hormone loss (Navarro *et al.* 2008, Paradies *et al.* 2011, Hara *et al.* 2015).

The accumulation of oxidative products leading to changes in mitochondrial macromolecules has been proposed as a plausible mechanism underlying the aforementioned alterations induced by ovarian hormone loss and in aging (Paradies *et al.* 2011, Viña *et al.* 2011, López-Grueso *et al.* 2014). Mitochondrial membranes, mostly composed of phospholipids, are main targets of oxidative damage due to their physicochemical properties and the chemical reactivity of their fatty acid (FA) double bonds (Pamplona 2008, Paradies *et al.* 2011). In fact, membrane phospholipid unsaturation degree has been suggested to play a causal role in aging by modulating oxidative stress and molecular integrity of the membrane, which is particularly important for the proper activity of proteins involved in oxidative phosphorylation (Pamplona 2008, Schenkel & Bakovic 2014).

Similar to other subcellular membranes, phosphatidylcholine (PC) and phosphatidylethanolamine (PE) are the major phospholipids in mitochondrial membranes, comprising 40 % and 30 % of total mitochondrial phospholipids, respectively (Schenkel & Bakovic 2014). Unlike the plasma membrane, mitochondria contain high levels of cardiolipin (CL), a phospholipid localized almost exclusively in the inner mitochondrial membrane that is essential for several mitochondrial processes such as oxidative phosphorylation, apoptosis, mitochondrial protein import and

supercomplex formation (Claypool & Koehler 2012). Due to its location near the site of ROS production and to the fact that it is particularly rich in unsaturated FAs, brain CL is highly prone to oxidative attack (Pamplona 2008). During aging, both an increase in the levels of oxidized CL together with a reduction in CL content in brain mitochondria have been reported (Sen *et al.* 2007, Petrosillo *et al.* 2008, Jones & Brewer 2009), conditions that have been suggested to contribute to mitochondrial dysfunction in multiple aged tissues (Paradies *et al.* 2011). Studies on the putative association between ovarian hormone loss and alterations in mitochondrial membrane lipid profile, especially in CL, are still lacking.

In this context, the aim of this work was to assess bioenergetic alterations and mitochondrial membrane lipid profile induced by long-term ovarian hormone deprivation in the hippocampus, a highly hormone-responsive area primarily affected during aging. By doing so, we aimed to get a better understanding on how putative changes in mitochondrial phospholipid profile, especially in CL, are reflected in hippocampal mitochondria dysfunction usually associated with menopause.

Materials and Methods

Drugs

All drugs and chemicals were obtained from Sigma Chemical Co., St. Louis, MO, USA except for organic solvents (Carlo Erba, Milan, Italy), NAO and $DiOC_6$ (Molecular Probes, Eugene, OR, USA), phospholipid standards (Avanti Polar Lipids Inc., Alabama, USA) and the materials indicated below.

Animals

Adult female Wistar rats were kept in controlled conditions of light (12 h light-dark cycles) and temperature (20–22°C). Rats were fed standard lab chow and water ad libitum and kept in accordance with the National Institutes of Health Guide for the Care and Use of Laboratory

Animals. All the procedures were carried out in strict compliance with the ARRIVE and the Ethical Committee of the School of Medicine, University of Buenos Aires guidelines. Rats were ovariectomized (OVX) or sham-operated (SHAM) at three months of age under ketamine (100 mg/kg, i.p.) and xylazine (10 mg/kg, i.p.) anesthesia and ketoprofen (5 mg/kg) for analgesia. Two weeks before the experiments, rats were monitored daily by vaginal smears for normal 4-5 day estrous cycles (SHAM) or continuous diestrus status (OVX). Twelve weeks after the surgery, rats were subjected to behavioral tests and then euthanized in a CO_2 chamber followed by decapitation. Body and uteri weight were recorded. Brains were rapidly removed and hippocampi dissected on ice and immediately processed for mitochondrial isolation.

Behavioral tests

Open field test

The open field test (OFT) was performed to evaluate animal general locomotion and exploratory behavior. The arena consisted of a squared open field (70 x 70 cm) limited by a 40 cm-height wall with the floor divided in squares (15 × 15 cm) by lines. Animals were individually placed in the centre of the open field arena and were allowed to freely explore for 10 min. Locomotion was measured based on the number of lines crossed with all four paws (crossings). After each animal was tested, the open field was cleaned with a 10% v/v ethanol-damp cloth. Testing was performed between 10:00 and 14:00 h in a quiet room evenly illuminated with cool white lights situated above the center of the apparatus.

Forced swimming test

The forced swimming test (FST) was performed to evaluate animal depressive-like behaviors by quantifying their mobility, immobility and associated behaviors. The FST was performed 24-48 h after the animals were evaluated in the OFT. Each rat was individually placed in a plastic cylinder

(diameter, 40 cm; height, 35 cm) containing water (23−25°C) up to 25 cm from the bottom for 5 min. At 5 s intervals throughout the test session, the predominant behavior was assigned to one of the followings categories: (1) immobility: lack of movement, except for the ones needed to keep the head above water; (2) swimming: swimming movement throughout the cylinder or (3) climbing: vigorous movements of the forepaws in and out of the water, usually directed against the walls. After each animal was tested, the water was changed and the cylinder rinsed with clean water. Following the session, each animal was dried and replaced to its housing cage in a temperature-controlled room. All swimming sessions were carried out between 10:00 and 16:00 h.

Mitochondria isolation

Hippocampal mitochondria purified fractions were obtained from tissue homogenates by differential centrifugation (Martino Adami *et al.* 2015). Briefly, hippocampi were homogenized by five strokes in a glass–Teflon homogenizer in a medium containing 250 mM sucrose, 5 mM Tris–HCl and 2 mM EGTA (pH 7.4) and centrifuged at 700 x g for 10 min to discard nuclei and cell debris. Then, the supernatant was centrifuged at 8000 x g for 10 min and the enriched mitochondria pellet was resuspended in a minimum volume (250 µl) of the same buffer. The whole procedure was carried out at 4°C. The purity of isolated mitochondria was assessed by determining lactate dehydrogenase activity; only mitochondrial preparations with less than 5% impurity were used (Vanasco *et al.* 2014).

Mitochondrial membrane preparation

Mitochondrial membranes were obtained by three freeze-thaw cycles of the mitochondrial preparation, followed by a homogenization step by passage through a 29G hypodermic needle (Vanasco *et al.* 2014).

180

181 **Mitochondrial function**

182 **O_2 consumption**

183 Mitochondrial O_2 uptake was measured by high-resolution respirometry (Hansatech Oxygraph,
184 Hansatech Instruments Ltd, Norfolk, England). Briefly, fresh isolated mitochondria at a
185 concentration of 0.25-0.50 mg of protein/ml were incubated in an air-saturated respiration buffer
186 ($[O_2]$=220 µM) containing 120 mM KCl, 5 mM KH_2PO_4, 1 mM EGTA, 3 mM HEPES and 1 mg/mL
187 fatty acid-free BSA (pH 7.4) at 30°C. State 4 respiration rates (resting or controlled respiration)
188 were determined using 6 mM malate and 6 mM glutamate or 7 mM succinate as substrates of
189 complex I or II, respectively; ADP (125 µM) was added to trigger state 3 (active respiration).
190 Respiratory control ratio (RCR) was calculated as the ratio of state 3/state 4 respiration rates.
191 Then, 2 µM oligomycin (Fo-F1 ATP synthase inhibitor) was added to reach 4oligomycin (state 4_O)
192 respiration, followed by the protonophore carbonyl cyanide m-chlorophenylhydrazone (m-CCCP)
193 (2 µM) to evaluate mitochondrial uncoupled respiration (state 3_u) (Brand & Nicholls 2011). Results
194 were expressed as ng-at O/min.mg protein.

195 **ATP production rate and P/O ratio**

196 Mitochondrial ATP production rate was determined using a chemiluminescence assay based on
197 the luciferin–luciferase system. Freshly purified mitochondria were incubated in respiration buffer
198 (150 mM KCl, 25 mM Tris–HCl, 2 mM EDTA, 0.1% (w/v) BSA and 100 µM MgCl2, pH 7.4) in the
199 presence of 40 µM d-luciferin, 0.05 µg/ml luciferase and 150 µM di(adenosine) pentaphosphate.
200 ATP production was triggered by the addition of 6 mM malate and 6 mM glutamate or 7 mM
201 succinate and 125 mM ADP to the reaction well (Drew & Leeuwenburgh 2003).
202 Chemiluminescence was measured at 30°C using a Labsystems Luminoskan RS Microplate Reader
203 (Labsystem, Ramsey, Minnesota, USA) using ATP as standard. A negative control with 2 µM

oligomycin was included to confirm that the emitted chemiluminescence was due to ATP synthesis by the Fo-F1 ATP synthase. Results were expressed as nmol ATP/min.mg protein. In order to evaluate the efficiency of the oxidative phosphorylation process, the number of phosphorylated ADP molecules per oxygen atom (P/O ratio) was calculated as ATP production/state 3 O_2 consumption rates (Brand & Nicholls 2011).

Membrane potential (ΔΨm)

Freshly isolated mitochondria (100 µg protein/ml) were incubated with the potentiometric cationic probe 3,3′-dihexyloxacarbocyanine iodide ($DiOC_6$, 30 nM) in respiration buffer in the dark at 37°C for 20 min. After the incubation period, mitochondria were analyzed by flow cytometry using a Partec PAS-III flow cytometer (Partec GmbH, Münster, Germany). Mitochondria were gated based on light-scattering properties and 30,000 events within this gate per sample were collected for analysis. 10-N-nonyl acridine orange (NAO, 100 nM) was used to selectively stain mitochondria through binding cardiolipin and evaluate the purity of mitochondrial preparations. $DiOC_6$ signal was analyzed after the addition of 6 mM malate and 6 mM glutamate (state 4) and 125 mM ADP (state 3) to the reaction mixture and the arithmetic mean values of the median fluorescence intensities (MFI) were obtained. Total depolarization induced by 2 µM m-CCCP was used as a positive control. Mitochondrial preparations that showed no changes in membrane potential under this condition were discarded. Analysis of the data was performed using Cyflogic software (Magnani *et al.* 2013).

Respiratory chain complex activity

NADH-cytochrome c reductase (complexes I-III) and succinate cytochrome c reductase (complexes II-III) activities were evaluated by a colorimetric assay following cytochrome c^{3+} reduction rate at 550 nm and 30°C using a spectrophotometer (Beckman DU 7400; ε = 19 mM^{-1} cm^{-1}). Mitochondrial membranes (1.0 mg protein/ml) were added to 100 mM phosphate buffer (pH 7.2),

supplemented with 0.2 mM NADH or 5 mM succinate respectively, plus 25 µM cytochrome c^{3+} and 0.5 mM KCN. Results were expressed as nmol reduced cytochrome c^{3+}/min.mg protein. Cytochrome oxidase (complex IV) activity was determined at 30°C in 100 mM phosphate buffer containing freshly prepared 60 µM cytochrome c^{2+}. The rate of cytochrome c^{2+} oxidation was calculated as the pseudo-first-order reaction constant k′/min.mg protein.

Lipid analysis

Global fatty acid composition of mitochondrial membranes and major phospholipid profile analysis

Total lipids from an aliquot of mitochondrial membranes containing 0.5 mg of protein were extracted by the method of Folch et al. (Folch *et al.* 1957), dried under N_2 and saponified with KOH 10 % v/v in ethanol (30 min at 85°C). Unsaponified compounds were extracted with hexane. The aqueous phase was acidified with HCl 37 % v/v and extracted twice with hexane. Both hexane phases were dried under N_2 and FA methyl esters (FAMEs) were synthesized by incubating in BF_3 10 % v/v in methanol 1 h at 85°C. The resulting FAMEs were extracted with hexane and used to analyze the global FA composition of mitochondrial membranes.

In parallel, total lipids from an aliquot of mitochondrial membranes containing 2 mg of protein were extracted as described above. Phospholipids were separated by 2-D high-performance thin layer chromatography (HPTLC) on pre-coated silica gel plates (10 x 20 cm) from Whatman Schleicher and Schuell (Maidstone, England). The mobile phase for the first-D was chloroform:methanol:water:amonium hidroxide: (65:25:4:0.5, by volume) and the mobile phase for the second-D was chloroform:acetone:methanol:acetic acid:water (36:48:12:12:6, by volume). Spots were visualized by iodine vapor. CL, PC and PE were identified by comparison with commercial standards and quantified by densitometric analysis using Image J sofware (NIH). CL, PC

and PE spots were scrapped off the plate and extracted from the silica with chloroform:methanol (1:2 v/v). The extracts were dried under N_2, saponified and used to obtain FAMEs as described above to analyze the FA composition of each mitochondrial phospholipid.

FAMEs analysis was performed by Gas-liquid chromatography using a capillary column (Omegawax 250) mounted on a Hewlett Packard HP 6890 Series GC System Plus (Avondale, PA, USA). FAMEs were identified by comparison of their relative retention times with authentic standards and mass distribution was calculated by quantification of the peak areas and expressed as relative quantity of each FAME from the total FAMEs in the sample. Peroxidizability index (PI) was calculated as (% monoenoic acids x 0.025) + (% dienoic acids x 1) + (% trienoic acids x 2) + (% tetraenoic acids x 4) + (pentaenoic acids x 6) + (hexaenoic acid x 8) (Pamplona 2008).

Cholesterol content

Cholesterol (CHOL) content was determined enzymatically using a commercial kit (Wienner Lab., Rosario, Argentina).

Protein measurements

Protein content was determined by the Bradford protein assay (BioRad Laboratories, CA, USA) or the method of Lowry et al. (Lowry *et al.* 1951), using bovine serum albumin as standard.

Statistical analysis

Results are expressed as mean ± SEM and evaluated by unpaired Student's t test. The "n" in each experiment corresponds to the number of animals used. Differences were considered significant if $p < 0.05$.

Results

Ovariectomy validation parameters

Previous reports have shown that ovarian hormone depletion induces depression-like effects in both young and middle-aged rats (Diz-Chaves *et al.* 2012, Kiss *et al.* 2012, da Silva Moreira *et al.* 2016). We thus evaluated animal performance in the FST as an independent indicator for the efficacy of experimental ovariectomy in our model. Twelve-week ovarian hormone deprivation increased despair behavior in OVX rats, evidenced by an increase in the time spent immobile in the FST (Fig. 1 A). Analysis of the animals' performance in the OFT did not show any difference in spontaneous locomotion between OVX and SHAM groups, indicating that the increased immobility time was not due to changes in locomotor activity (Fig. 1 B). Uterine weight was also used as a bioassay to verify the efficacy of long-term ovarian hormone deprivation induced by ovariectomy. As expected, OVX rats showed a decrease in uterine weight relative to body weight when compared with SHAM rats (Fig. 1 C).

Mitochondrial function

Mitochondrial O_2 uptake and ATP production rates

Increasing evidence indicates that brain mitochondria are targets of gonadal steroid action and, consequently, ovarian hormone loss during reproductive senescence has been associated with whole brain energetic deficits (Yao *et al.* 2012, Velarde 2014). We evaluated different parameters of mitochondrial function in isolated hippocampal mitochondria from long-term OVX rats. We firstly measured oxygen consumption using NADH-dependent substrates malate-glutamate. Representative traces are shown in Fig. 2. While ovariectomy did not affect the rate of resting respiration, it significantly decreased mitochondrial respiration in the active state (i.e. the respiratory activity that sustains ATP formation) (Table 1). We further assessed mitochondrial respiration in the presence of the Fo-F1 ATP synthase inhibitor oligomycin and the protonophore

m-CCCP. Inhibition of ATP synthesis by oligomycin (state 4_o) yielded a slower respiration rate while uncoupling by m-CCCP (state 3_u) accelerated the rate of oxygen consumption (Table 1). No differences between groups were observed in state 4_o respitation rate, which mainly reflects proton leak. Also, since state 3_u is exclusively dependent on substrate oxidation and electron transfer rates, no differences between groups may indicate lack of inhibition at the mitochondrial electron transport chain. On the other hand, ATP production rate was lower in hippocampal mitochondria from OVX rats (Fig. 3). Calculation of the P/O ratio showed no differences between groups, indicating that the lower chemical energy production in mitochondria from OVX rats is due to the observed decreased state 3 oxygen uptake rather than a hindered oxidative phosphorylation (Table 1).

Unlike what was observed for NADH-associated respiration, there were no differences in either active or basal respiration or ATP production rates between the experimental groups when $FADH_2$-linked respiration was promoted by using succinate as a substrate for complex II (Table 1 and Fig. 3).

Mitochondrial membrane potential (ΔΨm)

We then evaluated mitochondrial membrane potential (Δψm), the charge gradient across the inner mitochondrial membrane that ultimately regulates ATP production. Isolated hippocampal mitochondria were selected from background by light-scattering and NAO binding properties (Fig. 4 A, B). As it is shown in the overlaid histograms and $DIOC_6$ MFI quantification, hippocampal mitochondria from OVX rats showed no changes in Δψm during resting respiration (Fig. 4 C, D). However, when active respiration was established, OVX Δψm was lower than SHAM Δψm, indicating a significant depolarization in isolated mitochondria from long-term ovarian hormone deprived rats (Fig. 4 C, D).

Mitochondrial respiratory chain complex activity

In order to study the source for this mitochondrial dysfunction with shortage of energy supply, we evaluated the enzymatic activity of respiratory complexes in mitochondrial membranes. We found no differences in the activity of any of the complexes, as shown in Table 2.

Mitochondrial lipid analysis

Lipid composition and fatty acid profile of mitochondrial membranes

The observed bioenergetics deficits in hippocampal mitochondria from OVX rats may be related to an altered lipid composition of mitochondrial membranes. Thus, we analyzed lipid components of mitochondrial membranes, including cholesterol (CHOL), FA composition as well as content and FA composition of main individual phospholipids. Total lipids were extracted from hippocampal mitochondrial membranes of OVX and SHAM rats and CHOL content was determined. As shown in Fig. 5 A, CHOL levels were similar between the two groups (Fig. 5 A). On the other hand, we found that long-term ovarian hormone deprivation altered the FA profile of mitochondrial membranes by decreasing the proportion of saturated palmitic (16:0) and unsaturated oleic (18:1 n-9) acids together with increasing saturated arachidic (20:0) and polyunsaturated (PUFA) arachidonic (20:4 n-6) acids (Fig. 5 B). This FA composition led to a higher peroxidizability index (PI) in hippocampal mitochondrial membranes from OVX rats (Fig. 5 C).

Mitochondrial phospholipid content and phospholipid FA profile

In parallel, phospholipids were isolated from lipid extracts by HPTLC fractionation and the relative abundance of CL, PC and PE were assessed. Long-term ovarian hormone deprivation promoted a significant decrease (20 %) in CL content without changes in the levels of PC or PE (Fig. 6 A). The analysis of the FA profile for each phospholipid showed that CL from hippocampal mitochondria from OVX rats contained an increased proportion of saturated palmitic acid and such a profile for PUFAs leading to a lower PI for this phospholipid. A similar result was observed for PC. On the

other hand, PE showed a higher proportion of docosatetraenoic (22:4) and docosahexaenoic (22:6) acids leading to a higher PI (Fig. 6 B, C). These results show that long-term ovarian hormone deprivation alters the FA composition within major mitochondrial phospholipids and suggest that PE accounts for the higher global PI of hippocampal mitochondrial membranes.

Discussion

The brain consumes 20 % of the body fuel to sustain its high demand of energy in the form of ATP and thus is particularly susceptible to a bioenergetic decline if mitochondrial function is impaired (Rettberg *et al.* 2014). Multiple epidemiologic studies reported that women are more prone to develop dementia and Alzheimer's disease than men (Gao *et al.* 1998, Zandi *et al.* 2002, Andersen *et al.* 1999, Fratiglioni *et al.* 1997), suggesting a strong link with the drop in circulating ovarian hormones during menopause and reduced brain bioenergetics (Maki & Resnick 2000, Rasgon *et al.* 2005). Studies in animals undergoing natural or surgical reproductive senescence have also shown a decline in the bioenergetic system of the brain, from decreased glucose metabolism to impaired mitochondrial function (Yao *et al.* 2009, Yao *et al.* 2010, Yao *et al.* 2012). However, most - if not all - of these studies have been performed in the whole brain. Considering the variety and complexity of metabolic conditions in different brain areas, we chose to perform this study in the hippocampus for its exceptional vulnerability to the detrimental effects of aging and loss of ovarian hormones (Navarro *et al.* 2008, Paradies *et al.* 2011, Hara *et al.* 2015). Evidence supporting this fact comes from several studies showing synaptic decline in this brain area associated with cognitive impairment and increased risk of neurodegeneration after experimental endocrine senescence in animal models and menopause in women (Morrison *et al.* 2006, Brinton 2009, Velarde 2014, Hara *et al.* 2015). Also, a more marked mitochondrial dysfunction is observed in the hippocampus than in brain cortex or whole brain, and oxidative damage is higher in the

hippocampus than in whole brain in male rodents during aging (Navarro *et al.* 2008). Moreover, ovariectomy induces a sharp decrease in the activity of the antioxidant enzyme superoxide dismutase in the hippocampus but not in the cortex of young rats (Huang & Zhang 2010).

Our results show that long-term ovarian hormone deprivation induces a decline in mitochondrial bioenergetics in the hippocampus, specifically a reduction in active respiration and ATP production rates without changes in the rate of basal respiration with NADH-dependent substrates. Also, membrane depolarization was only observed during active respiration, which could account for the decrease in ATP production rate in hippocampal mitochondria from OVX rats. This lower membrane potential may indicate a defective formation of a proper proton gradient across the inner mitochondrial membrane (IMM) during active respiration in mitochondria from OVX rats. Our results are in line with those obtained in isolated mitochondria from whole brain in OVX mice, in which ovariectomy induced a deficit in state 3 respiration without altering state 4 respiration both in wild type mice and in the 3xTg-AD mouse model of Alzheimer's disease (Yao *et al.* 2012). On the other hand, $FADH_2$-linked respiration, either active or basal, was not affected by ovarian hormone loss, suggesting the involvement of complex I alterations in mitochondrial dysfunction. One possible explanation for altered complex I function could be a reduction in its activity. Indeed, mitochondrial dysfunction in terms of reduced complex I and IV enzymatic activities and decreased mitochondrial respiration with NADH-dependent substrates has been consistently observed in brain mitochondria from aged rats and mice (Navarro & Boveris 2004, Navarro *et al.* 2005, Cocco *et al.* 2005). Also, decreased bioenergetics in synaptic mitochondria from whole brain is mainly associated with a decay in complex I activity in 3xTg-AD mice at an early, pre-symptomatic stage of the disease (Monteiro-Cardoso *et al.* 2015). However, our results show no changes in the enzymatic activity of any of the respiratory complexes and are in agreement with those obtained in a recent report in whole brain mitochondria from OVX mice (Gaignard *et al.*

2015). The apparent discrepancy between decreased mitochondrial respiration in state 3 when using NADH-related substrates in intact mitochondria and lack of differences in complex I-III enzymatic activity evaluated in mitochondrial membrane preparations could be methodological in nature. It has been reported that freeze-thawing cycles to obtain preparations of mitochondrial membranes alter the organization of the IMM complexes, allowing detection of the activity of only individual complexes or smaller aggregates (Parenti *et al.* 1987). These smaller aggregates would exhibit less efficient collision-based electron transport behavior instead of stoichiometric behavior, characterized by kinetically advanced substrate/electron channeling, observed in the presence of supercomplexes in intact mitochondria (Lenaz & Genova 2007, Genova & Lenaz 2014). It can thus be hypothesized that, when assessing complex I-III activity in mitochondrial membrane preparations, NADH oxidation is less efficient and thus no changes are found in complex I-III activity between experimental groups.

Also, defects in complex I substrate transport could account for the involvement of complex I alterations in mitochondrial dysfunction induced by hormone deprivation. It is well established that the respiratory rate in State 3 is limited not only by the activity of the individual complexes of the respiratory chain, but also by substrate permeation and adenine nucleotide translocation. The decreased state 3 respiration rate with malate-glutamate in brain mitochondria from aged rats has been ascribed to glutamate uptake impairment that could involve the glutamate-OH antiporter or the glutamate/aspartate exchanger (Vitorica *et al.* 1985). Also, the low activity of the phosphate carrier, one of the transporters involved in the uptake of some of the Krebs-cycle intermediates such as malate, has been suggested to account for the decreased energy metabolism typically found in liver mitochondria during aging (Paradies *et al.* 1991). On the other hand, State 3 respiration rate when using succinate as a substrate was not significantly modified, indicating that succinate permeation and oxidation were not altered in brain mitochondria from old rats (Vitorica

420 *et al.* 1985). Although the ADP/ATP carrier is also a major regulator of state 3 respiration, the fact
421 that succinate-induced active oxygen uptake is not altered in hormone-deprived animals makes
422 very unlikely for impaired ADP uptake as the cause of decreased NADH-linked bioenergetic
423 capacity. Further experiments are needed to test whether ovarian hormone loss impairs the
424 aforementioned complex I substrate transporters.
425 A further explanation for the observed ovariectomy-related complex I alterations leading to
426 mitochondrial dysfunction is that the lipid milieu of the IMM may be altered due to ovarian
427 hormone loss. An altered IMM is expected to influence the stability and activity of the proteins
428 embedded in it, both respiratory complexes and substrate carriers (Gómez & Hagen 2012, Vitorica
429 *et al.* 1985). Our results show that long-term ovarian hormone deprivation induces changes in the
430 FA profile of mitochondrial membranes that renders them more prone to peroxidation, indicated
431 by a higher PI. This fact may alter membrane fluidity while cholesterol levels remain the same
432 (Choe *et al.* 1995). Although a relative increase in the PUFA content of a membrane would be
433 expected to render it more fluid, the opposite has been systematically reported during aging;
434 membrane fluidity decreases while PI increases with age (Hulbert *et al.* 2007, Naudí *et al.* 2013). A
435 possible explanation for this paradox is that PUFAs, being more vulnerable to oxidative attack,
436 experience greater lipid oxidative damage and the resulting endoperoxide reactive intermediates
437 have been reported to significantly contribute to membrane rigidity and loss of membrane
438 function (Naudí *et al.* 2013). Indeed, it has been suggested that the age-related decrease in
439 mitochondrial membrane fluidity can have a considerable impact on the activity of the respiratory
440 complexes as well as the generation of the proton gradient (Kwong & Sohal 2000). Aged-induced
441 mitochondrial transporter deficiencies have been suggested to be due to either a general
442 alteration of membrane lipid composition/fluidity or to a more confined change in the lipid milieu
443 surrounding carrier molecules in the IMM, such as a lower content of cardiolipin (Paradies *et al.*

1991, Vitorica *et al.* 1985). Aged-related modifications in the IMM lipid content and composition have been broadly reported as causing a deleterious effect in membrane structural organization, which in turn contributes to mitochondrial dysfunction (Gómez & Hagen 2012). Particularly, membrane unsaturation degree has been extensively related to aging. An increase in membrane PI and lipid peroxidation during aging in an organ-dependent manner have also been reported (Pamplona 2008). Thus, our results suggest that ovarian hormone loss induces a mitochondrial phenotype similar to an aging-related one in terms of higher susceptibility to membrane peroxidation concomitant with impaired mitochondrial bioenergetic capacity.

Among a variety of factors, both ovarian hormones and aging have been shown to regulate the expression of elongases and desaturases, which together with the peroxisomal beta-oxidation pathway, are involved in the production of all the diversity of FAs present in a cellular membrane (Naudí *et al.* 2013, Xu *et al.* 2007, Marks *et al.* 2013, Stark *et al.* 2003). The expression of elongase 6, which preferentially elongates saturated fatty acids such as 16:0 palmitic acid, is increased specifically in the hippocampus of old mice and is considered an aging associated gene (Xu *et al.* 2007). In addition, the expression of this enzyme increases in the liver of OVX animals (Marks *et al.* 2013). Postmenopausal women have a lower percentage of 16:0 in serum phospholipids as compared with premenopausal women and postmenopausal women receiving hormone therapy (Stark *et al.* 2003). In addition, the protein expression of stearoyl-CoA desaturase 1 (SCD1), involved in the generation of 18:1 n-9 by delta-9 desaturation of 18:0, is higher in the liver of estradiol and progesterone-treated rats, suggesting that ovarian hormones are implicated in MUFA biosynthesis through elongase 6 and SCD1 (Marks *et al.* 2013). Interestingly, we observed decreased levels of 16:0 and 18:1 n-9 in mitochondria membranes from OVX rats, suggesting that ovarian hormones may also be involved in MUFA biosynthesis through these enzymes in the hippocampus. Regarding PUFA biosynthesis, ovariectomy has been reported to increase the

transcript levels of hepatic Δ6- and Δ5-desaturases (Alessandri *et al.* 2011). Notably, we observed that ovarian hormone deprivation increased the levels of 20:4 and 22:6 FAs, which can be generated as the products of Δ6- and Δ5-desaturases. It can therefore be speculated that ovarian hormone loss may promote a higher PI in mitochondria membranes through the modulation of the expression and/or activity of specific elongases and desaturases in the hippocampus.

Among membrane lipids, CL and PE are crucial for mitochondrial functions (Genova & Lenaz 2014). Due to their particular conical shape, they facilitate membrane bending and can provide order to surrounding lipids (Zeczycki *et al.* 2014). Modifications in the content, structure or acyl chain composition of CL and PE are expected to directly impact on the properties of the membrane and on the efficiency of the respiratory complexes. CL is almost exclusively located in the IMM, where it is critical for the proper folding and functioning of a number of proteins playing an important role in mitochondrial bioenergetic processes (Raja & Greenberg 2014). A significant decline in CL content, alterations in its acyl chain composition, and/or CL peroxidation have been associated with mitochondrial dysfunction in multiple tissues during aging as well as in a variety of pathological conditions, including ischemia, hypothyroidism, heart failure and Alzheimer's disease (Gómez & Hagen 2012, Paradies *et al.* 2014, Monteiro-Cardoso *et al.* 2015). Our present data from HPTLC fractionation of mitochondrial phospholipids showed a specific decrease in CL content in hippocampal mitochondria from OVX rats, suggesting that ovarian hormones may be involved in the maintenance of CL levels. In fact, in vitro 17β-estradiol treatment prevents age-related loss of CL and improves neuronal respiration in response to glutamate in cultured aging neurons (Jones & Brewer 2009). Alterations in normal CL biosynthesis and remodeling have been associated with numerous pathological situations. It has been reported that failures in CL remodeling leads to decreased CL content due to reduced stability or increased degradation of CL with abnormal side chain composition, which is shifted towards more saturated species (Lu & Claypool 2015).

Interestingly, we observed that ovariectomy induced an altered CL fatty acid profile characterized by increased levels of saturated palmitic acid and reduced levels in PUFAs, suggesting that ovarian hormone loss may alter CL remodeling and/or increase CL oxidation resulting in the observed FA profile. Similarly, PC FA profile showed decreased PUFA levels, resulting in a lower PI. On the other hand, the opposite was observed for PE FA profile, with increased levels of PUFAs resulting in a higher PI, which could account for the general higher PI of hippocampal mitochondria membranes from OVX rats. It can be speculated that alterations in CL remodeling, which uses PC or PE as substrates for FA transacylation, could explain the altered phospholipid FA profiles found in long-term hormone deprived animals. Despite that sequences of estrogen responsive elements have been found in the promoters of enzymes involved in CL remodeling (E Acaz-Fonseca, A B Lopez-Rodriguez, A Ortiz-Rodriguez, L M Garcia-Segura & M Astiz, unpublished observations), further analysis of these pathways should be performed to test this hypothesis.

Extensive evidence indicates that, in addition to affecting the stability and catalytic activity of individual complexes, CL stabilizes respiratory supercomplexes, quaternary supramolecular structures that favor efficient electron transfer by directly transferring electrons among individual complexes without its diffusion in the bulk medium (Gómez & Hagen 2012, Genova & Lenaz 2014). Moreover, it has been reported that the stability of complex I is highly dependent on its assembly within the respiratory supercomplex (Genova & Lenaz 2014). The interactions between membrane lipids and proteins in the IMM are key to maintaining supercomplex stability. It has been suggested that altered CL acyl chain content induces age-related destabilization of brain cortical supercomplexes (Frenzel *et al.* 2010). Therefore, alterations induced by ovarian hormone deprivation in CL content and/or its FA composition could compromise the stability of respiratory supercomplexes that, in turn, would affect the stability of complex I leading to decreased active respiration with NADH-linked substrates in hippocampal mitochondria. In fact, it has been

reported that supercomplexes are dispensable for maintaining basal respiration but essential for supporting active respiration and bioenergetic reserve capacity (Gómez & Hagen 2012). Since complex I needs to be assembled into the NADH oxidase supercomplex for its optimal redox activity (Stroh *et al.* 2004), it can be speculated that reduced complex I redox energy leads to lower proton translocation across the inner mitochondrial membrane, resulting in lower membrane potential and decreased respiration with NADH-dependent substrates. Moreover, mitochondrial dysfunction and deficiency of respiratory supercomplexes are correlated to the mitochondrial aging phenotype and in the etiopathology of several diseases like Parkinson's and Alzheimer's (Seelert *et al.* 2009, Frenzel *et al.* 2010, Kuter et al 2016). On the other hand, complex II does not form part of respiratory supercomplexes, which is in agreement with lack of alterations in $FADH_2$-linked respiration and further supports the putative involvement of supercomplex destabilization induced by loss of ovarian hormones.

Taken together, our data support the hypothesis that hippocampal mitochondria dysfunction in terms of bioenergetic decay and altered mitochondria membrane phospholipid composition are interconnected players contributing to the early bioenergetic decay during menopause. It has been previously suggested that loss of ovarian hormones precipitates the decline in mitochondrial bioenergetics promoting an accelerated aging phenotype eventually leading to the development of brain hypometabolism, which is clinically observed in menopausal women and prodromal Alzheimer's disease brains (Yao *et al.* 2009). Our data agrees with and further expands this hypothesis in terms of the aging effects of ovarian hormone loss in mitochondrial membrane composition. In line with this, the maintenance of membrane properties emerges as a putative therapeutic target worth exploring to avoid early impairments in mitochondrial energy expenditure that affects the high-energy demanding brain after ovarian hormone natural or surgical loss.

Declaration of interest: The authors declare that there is no conflict of interest that could be perceived as prejudicing the impartiality of the research reported.

Funding

This study was supported by ANPCYT (PICT 2014-1549 and PICT 2014-0334), CONICET (PIP 0159 and PIP 0321) and UBA (UBACyT (2013-2016) 20020120300064BA and UBACYT (2014-2017) 20020130100786). The funders had no role in study design, data collection and analysis, decision to publish or preparation of the manuscript.

Acknowledgements

We would like to thank Dr. Daniel Pisera for critical reading of the manuscript and Dr. Martin Codagnone for his helpful assistance with behavioral tests.

References

1. Alessandri JM, Extier A, Al-Gubory KH, Langelier B, Baudry C, LePoupon C, Lavialle M & Guesnet P 2011 Ovariectomy and 17beta-estradiol alter transcription of lipid metabolism genes and proportions of neo-formed n-3 and n-6 long-chain polyunsaturated fatty acids differently in brain and liver. *J Nutr Biochem* **22**:820–827.
2. Andersen K, Launer LJ, Dewey ME, Letenneur L, Ott A, Copeland JR, Dartigues JF, Kragh-Sorensen P, Baldereschi M, Brayne C et al 1999 Gender differences in the incidence of AD and vascular dementia: the EURODEM Studies. EURODEM Incidence Research Group. *Neurology* **53**:1992-1997.

3. Arnold S, Victor MB & Beyer C 2012 Estrogen and the regulation of mitochondrial structure and function in the brain. *J Steroid Biochem Mol Biol* **131**:2-9.
4. Brand MD & Nicholls DG 2011 Assessing mitochondrial dysfunction in cells. *Biochem J* **435**: 297-312.
5. Brinton RD 2009 Estrogen-induced plasticity from cells to circuits: predictions for cognitive function. *Trends Pharmacol Sci* **30**:212-222.
6. Chakrabarti S, Munshi S, Banerjee K, Thakurta IG, Sinha M & Bagh MB 2011 Mitochondrial dysfunction during brain aging: role of oxidative stress and modulation by antioxidant supplementation. *Aging Dis* **2**:242-256.
7. Choe M, Jackson C & Yu BP 1995 Lipid peroxidation contributes to age-related membrane rigidity. *Free Radic Biol Med* **18**:977-984.
8. Claypool SM & Koehler CM 2012 The complexity of cardiolipin in health and disease. *Trends Biochem Sci* **37**:32-41.
9. Cocco T, Sgobbo P, Clemente M, Lopriore B, Grattagliano I, Di Paola M & Villani G 2005 Tissue-specific changes of mitochondrial functions in aged rats: effect of a long-term dietary treatment with N-acetylcysteine. *Free Radic Biol Med* **38**:796-805.
10. da Silva Moreira SF, Nunes EA, Kuo J, de Macedo IC, Muchale A, de Oliveira C, Scarabelot VL, Marques Filho PR, Medeiros LF, Caumo W *et al.* 2016 Hypoestrogenism alters mood: Ketamine reverses depressive-like behavior induced by ovariectomy in rats. *Pharmacol Rep* **68**:109-115.
11. Diz-Chaves Y, Kwiatkowska-Naqvi A, Von Hülst H, Pernía O, Carrero P & Garcia-Segura LM 2012 Behavioral effects of estradiol therapy in ovariectomized rats depend on the age when the treatment is initiated. *Exp Gerontol* **47**:93-99.

12. Drew B & Leeuwenburgh C 2003 Method for measuring ATP production in isolated mitochondria: ATP production in brain and liver mitochondria of Fischer-344 rats with age and caloric restriction. *Am J Physiol Regul Integr Comp Physiol* **285**:1259-1267.
13. Folch J, Lees M & Sloane Stanley GH 1957 A simple method for the isolation and purification of total lipids from animal tissues. *J Biol Chem* **226**:497-509.
14. Fratiglioni L, Viitanen M, von Strauss E, Tontodonati V, Herlitz A & Winblad B 1997 Very old women at highest risk of dementia and Alzheimer's disease: incidence data from the Kungsholmen Project, Stockholm. *Neurology* **48**:132-138.
15. Frenzel M, Rommelspacher H, Sugawa MD & Dencher NA 2010 Ageing alters the supramolecular architecture of OxPhos complexes in rat brain cortex. *Exp Gerontol* **45**:563-572.
16. Gaignard P, Savouroux S, Liere P, Pianos A, Thérond P, Schumacher M, Slama A & Guennoun R 2015 Effect of Sex Differences on Brain Mitochondrial Function and Its Suppression by Ovariectomy and in Aged Mice. *Endocrinology* **156**:2893-2904.
17. Gao S, Hendrie HC, Hall KS & Hui S 1998 The relationships between age, sex, and the incidence of dementia and Alzheimer disease: a meta-analysis. *Arch Gen Psychiatry* **55**:809-815.
18. Genova ML & Lenaz G 2014 Functional role of mitochondrial respiratory supercomplexes. *Biochim Biophys Acta* **1837**:427-443.
19. Gómez LA & Hagen TM 2012 Age-related decline in mitochondrial bioenergetics: does supercomplex destabilization determine lower oxidative capacity and higher superoxide production? *Semin Cell Dev Biol* **23**:758-767.
20. Hara Y, Waters EM, McEwen BS & Morrison JH 2015 Estrogen Effects on Cognitive and Synaptic Health Over the Lifecourse. *Physiol Rev* **95**:785-807.

21. Huang YH & Zhang QH 2010 Genistein reduced the neural apoptosis in the brain of ovariectomised rats by modulating mitochondrial oxidative stress. *Br J Nutr* **104**:1297-1303.
22. Hulbert AJ, Pamplona R, Buffenstein R & Buttemer WA 2007 Life and death: metabolic rate, membrane composition and lifespan of animals. *Physiol Rev* **87**:1175-1213.
23. Irwin RW, Yao J, Ahmed SS, Hamilton RT, Cadenas E & Brinton RD 2011 Medroxyprogesterone acetate antagonizes estrogen up-regulation of brain mitochondrial function. *Endocrinology* **152**:556-567.
24. Johri A & Beal MF 2012 Mitochondrial dysfunction in neurodegenerative diseases. *J Pharmacol Exp Ther* **342**:619-630.
25. Jones TT & Brewer GJ 2009 Critical age-related loss of cofactors of neuron cytochrome C oxidase reversed by estrogen. *Exp Neurol* **215**:212-219.
26. Kiss A, Delattre AM, Pereira SI, Carolino RG, Szawka RE, Anselmo-Franci JA, Zanata SM & Ferraz AC 2012 17β-estradiol replacement in young, adult and middle-aged female ovariectomized rats promotes improvement of spatial reference memory and an antidepressant effect and alters monoamines and BDNF levels in memory- and depression-related brain areas. *Behav Brain Res* **227**:100-108.
27. Kuter K, Kratochwil M, Berghauzen-Maciejewska K, Głowacka U, Sugawa MD, Ossowska K & Dencher NA 2016 Adaptation within mitochondrial oxidative phosphorylation supercomplexes and membrane viscosity during degeneration of dopaminergic neurons in an animal model of early Parkinson's disease. *Biochim Biophys Acta* **1862**:741-753.
28. Kwong LK & Sohal RS 2000 Age-related changes in activities of mitochondrial electron transport complexes in various tissues of the mouse. *Arch Biochem Biophys* **373**:16-22.

632 29. Lenaz G & Genova ML 2007 Kinetics of integrated electron transfer in the mitochondrial
633 respiratory chain: random collisions vs. solid state electron channeling. *Am J Physiol Cell*
634 *Physiol* **292**:C1221-1239.
635 30. López-Grueso R, Gambini J, Abdelaziz KM, Monleón D, Díaz A, El Alami M, Bonet-Costa V,
636 Borrás C & Viña J 2014 Early, but not late onset estrogen replacement therapy prevents
637 oxidative stress and metabolic alterations caused by ovariectomy. *Antioxid Redox Signal*
638 **20**:236-246.
639 31. Lowry OH, Rosebrough NJ, Farr AL & Randall RJ 1951 Protein measurement with the Folin-
640 phenol reagent. *J Biol Chem* **193**:265-275.
641 32. Lu YW & Claypool SM 2015 Disorders of phospholipid metabolism: an emerging class of
642 mitochondrial disease due to defects in nuclear genes. *Front Genet* **6**:3.
643 33. Magnani ND, Marchini T, Vanasco V, Tasat DR, Alvarez S & Evelson P 2013 Reactive oxygen
644 species produced by NADPH oxidase and mitochondrial dysfunction in lung after an acute
645 exposure to residual oil fly ashes. *Toxicol Appl Pharmacol* **270**:31-38.
646 34. Maki PM & Resnick SM 2000 Longitudinal effects of estrogen replacement therapy on PET
647 cerebral blood flow and cognition. *Neurobiol Aging* **21**:373-383.
648 35. Marks KA, Kitson AP, Shaw B, Mutch DM & Stark KD 2013 Stearoyl-CoA desaturase 1,
649 elongase 6 and their fatty acid products and precursors are altered in ovariectomized rats
650 with 17β-estradiol and progesterone treatment. *Prostaglandins Leukot Essent Fatty Acids*
651 **89**:89-96.
652 36. Martino Adami PV, Quijano C, Magnani N, Galeano P, Evelson P, Cassina A, Do Carmo S,
653 Leal MC, Castaño EM, Cuello AC *et al.* L 2016 Synaptosomal bioenergetic defects are
654 associated with cognitive impairment in a transgenic rat model of early Alzheimer's
655 disease. *J Cereb Blood Flow Metab*. In press. doi: 10.1177/0271678X15615132 .

37. Monteiro-Cardoso VF, Oliveira MM, Melo T, Domingues MR, Moreira PI, Ferreiro E, Peixoto F & Videira RA 2015 Cardiolipin profile changes are associated to the early synaptic mitochondrial dysfunction in Alzheimer's disease. *J Alzheimers Dis* **43**:1375-1392.

38. Morrison JH, Brinton RD, Schmidt PJ & Gore AC 2006 Estrogen, menopause, and the aging brain: how basic neuroscience can inform hormone therapy in women. *J Neurosci* **26**:10332-10348.

39. Naudí A, Jové M, Ayala V, Portero-Otín M, Barja G & Pamplona R 2013 Membrane lipid unsaturation as physiological adaptation to animal longevity. *Front Physiol* **4**:372.

40. Navarro A & Boveris A 2004 Rat brain and liver mitochondria develop oxidative stress and lose enzymatic activities on aging. *Am J Physiol Regul Integr Comp Physiol* **287**:R1244-1249.

41. Navarro A, Gomez C, Sanchez-Pino MJ, Gonzalez H, Bandez MJ, Boveris AD & Boveris A 2005 Vitamin E at high doses improves survival, neurological performance, and brain mitochondrial function in aging male mice. *Am J Physiol Regul Integr Comp Physiol* **289**:R1392-1399.

42. Navarro A, López-Cepero JM, Bández MJ, Sánchez-Pino MJ, Gómez C, Cadenas E & Boveris A 2008 Hippocampal mitochondrial dysfunction in rat aging. *Am J Physiol Regul Integr Comp Physiol* **294**:R501-509.

43. Pamplona R 2008 Membrane phospholipids, lipoxidative damage and molecular integrity: a causal role in aging and longevity. *Biochim Biophys Acta* **1777**:1249-1262.

44. Paradies G & Ruggiero FM 1991 Effect of aging on the activity of the phosphate carrier and on the lipid composition in rat liver mitochondria. *Arch Biochem Biophys* **284**:332-337.

45. Paradies G, Petrosillo G, Paradies V & Ruggiero FM 2011 Mitochondrial dysfunction in brain aging: role of oxidative stress and cardiolipin. *Neurochem Int* **58**:447-457.

679 46. Paradies G, Paradies V, De Benedictis V, Ruggiero FM & Petrosillo G 2014 Functional role of
680 cardiolipin in mitochondrial bioenergetics. *Biochim Biophys Acta* **1837**:408-417.
681 47. Parenti Castelli G, Fato R, Castelluccio C & Lenaz G 1987 Kinetic studies on the pool function
682 of ubiquinone in mitochondrial systems. *Chem Scr* **27**:161-166.
683 48. Petrosillo G, Matera M, Casanova G, Ruggiero FM & Paradies G 2008 Mitochondrial
684 dysfunction in rat brain with aging Involvement of complex I, reactive oxygen species and
685 cardiolipin. *Neurochem Int* **53**:126-131.
686 49. Raja V & Greenberg ML 2014 The functions of cardiolipin in cellular metabolism-potential
687 modifiers of the Barth syndrome phenotype. *Chem Phys Lipids* **179**:49-56.
688 50. Rasgon NL, Silverman D, Siddarth P, Miller K, Ercoli LM, Elman S, Lavretsky H, Huang SC,
689 Phelps ME & Small GW 2005 Estrogen use and brain metabolic change in postmenopausal
690 women. *Neurobiol Aging* **26**:229-235.
691 51. Rettberg JR, Yao J & Brinton RD 2014 Estrogen: a master regulator of bioenergetic systems
692 in the brain and body. *Front Neuroendocrinol* **35**:8-30.
693 52. Seelert H, Dani DN, Dante S, Hauss T, Krause F, Schäfer E, Frenzel M, Poetsch A, Rexroth S,
694 Schwassmann HJ *et al.* 2009 From protons to OXPHOS supercomplexes and Alzheimer's
695 disease: structure-dynamics-function relationships of energy-transducing membranes.
696 *Biochim Biophys Acta* **1787**:657-671.
697 53. Schenkel LC & Bakovic M 2014 Formation and regulation of mitochondrial membranes. *Int J*
698 *Cell Biol* **2014**:709828.
699 54. Sen T, Sen N, Jana S, Khan FH, Chatterjee U & Chakrabarti S 2007 Depolarization and
700 cardiolipin depletion in aged rat brain mitochondria: relationship with oxidative stress and
701 electron transport chain activity. *Neurochem Int* **50**:719-725.

55. Shi C, Zou J, Li G, Ge Z, Yao Z & Xu J 2011 Bilobalide protects mitochondrial function in ovariectomized rats by up-regulation of mRNA and protein expression of cytochrome c oxidase subunit I. *J Mol Neurosci* **45**:69-75.
56. Stark KD, Park EJ & Holub BJ 2003 Fatty acid composition of serum phospholipid of premenopausal women and postmenopausal women receiving and not receiving hormone replacement therapy. *Menopause* **10**:448-455.
57. Stroh A, Anderka O, Pfeiffer K, Yagi T, Finel M, Ludwig B & Schägger H 2004 Assembly of respiratory complexes I, III, and IV into NADH oxidase supercomplex stabilizes complex I in Paracoccus denitrificans. *J Biol Chem* **279**:5000-5007.
58. Vanasco V, Saez T, Magnani ND, Pereyra L, Marchini T, Corach A, Vaccaro MI, Corach D, Evelson P & Alvarez S 2014 Cardiac mitochondrial biogenesis in endotoxemia is not accompanied by mitochondrial function recovery. *Free Radic Biol Med* **77**:1-9.
59. Velarde MC 2014 Mitochondrial and sex steroid hormone crosstalk during aging. *Longev Healthspan* **3**:2.
60. Vitorica J, Clark A, Machado A & Satrústegui J 1985 Impairment of glutamate uptake and absence of alterations in the energy-transducing ability of old rat brain mitochondria. *Mech Ageing Dev* **29**:255-66.
61. Viña J, Gambini J, Lopez-Grueso R, Abdelaziz KM, Jove M & Borrás C 2011 Females live longer than males: role of oxidative stress. *Curr Pharm Des* **17**:3959-3965.
62. Xu X, Zhan M, Duan W, Prabhu V, Brenneman R, Wood W, Firman J, Li H, Zhang P, Ibe C *et al* 2007 Gene expression atlas of the mouse central nervous system: impact and interactions of age, energy intake and gender. *Genome Biol* **8**:R234.

63. Yao J, Irwin RW, Zhao L, Nilsen J, Hamilton RT & Brinton RD 2009 Mitochondrial bioenergetic deficit precedes Alzheimer's pathology in female mouse model of Alzheimer's disease. *Proc Natl Acad Sci U S A* **106**:14670-14675.

64. Yao J, Hamilton RT, Cadenas E & Brinton RD 2010 Decline in mitochondrial bioenergetics and shift to ketogenic profile in brain during reproductive senescence. *Biochim Biophys Acta* **1800**:1121-1126.

65. Yao J, Irwin R, Chen S, Hamilton R, Cadenas E & Brinton RD 2012 Ovarian hormone loss induces bioenergetic deficits and mitochondrial β-amyloid. *Neurobiol Aging* **33**:1507-1521.

66. Zandi PP, Carlson MC, Plassman BL, Welsh-Bohmer KA, Mayer LS, Steffens DC & Breitner JC 2002 Hormone replacement therapy and incidence of Alzheimer disease in older women: the Cache County Study. *JAMA* **288**:2123-2129.

67. Zeczycki TN, Whelan J, Hayden WT, Brown DA & Shaikh SR 2014 Increasing levels of cardiolipin differentially influence packing of phospholipids found in the mitochondrial inner membrane. *Biochem Biophys Res Commun* **450**:366-371.

Figure legends

Figure 1. **Evaluation of ovarian hormone depletion parameters in adult rats.** Adult Wistar female rats were ovariectomized (OVX) or sham-operated (SHAM). Twelve weeks after surgery, the animals were subjected to a 10-minute open field session followed by a 5-min forced swimming session 24 h later. Then, the animals were euthanized and body and uteri were weighed. (A) Forced swimming test: every 5 sec, a time-sampling technique was used to score the presence of immobility, swimming or climbing behavior. (B) SHAM or OVX rats were placed individually in the centre of a field marked with a grid of 12 equal squares for 10 min. The number of times the animal crossed each line was registered. (C) Animals' body and uterine weight were recorded. Each column represents the mean ± SEM of (A) the number of counts or (B) the number of crossings per session; (C) uterine weight relative to body weight (n=6-9 animals/group); *p<0.05, ***p<0.001, Student's t test.

Figure 2. Representative traces obtained during the assessment of mitochondrial O_2 uptake by hippocampal mitochondria from SHAM (thick, black line) and OVX (thin, grey line) rats. O_2 consumption was measured in resting (state 4) and active (state 3) metabolic states using malate-glutamate as complex I substrates and after the addition of 2 µM oligomycin (state 4_O) and 2 µM m-CCCP (state 3_U) to the reaction chamber.

Figure 3. ATP production rates of freshly isolated hippocampal mitochondria. ATP production rates were evaluated in isolated hippocampal mitochondria from SHAM and OVX rats by chemiluminescence. ATP production was triggered by the addition of malate-glutamate as complex I substrates or succinate as complex II substrate and ADP to the reaction chamber. Results are expressed as mean ± SEM (n=3-5 animals/group); *p<0.05, Student's t test.

Figure 4. Assessment of hippocampal mitochondria membrane potential (ΔΨm) by flow cytometry. Mitochondrial membrane potential in state 4 and 3 was evaluated in isolated hippocampal mitochondria from SHAM and OVX rats using the potentiometric cationic probe $DiOC_6$ and flow cytometry. (A) Representative dot blots when selecting hippocampal mitochondria from SHAM and OVX rats based on light scattering properties. (B) Representative histograms showing fluorescence of the events in the selected gate in (A) for NAO stained mitochondria (black line) compared to an unstained mitochondrial sample (grey line) in SHAM and OVX samples. (C) Representative histograms of $DiOC_6$ fluorescence from gated hippocampal mitochondria from SHAM and OVX rats. (D) $DiOC_6$ median fluorescence intensity (MFI) quantification of state 4 and state 3 in hippocampal mitochondria from SHAM and OVX rats. Each column represents the mean ± SEM of $DiOC_6$ MFI in resting (state 4) or active (state 3) respiration (n=4-6 animals/group). *p<0.05, Student's t test.

Figure 5. Cholesterol content, fatty acid composition and peroxidizability index of hippocampal mitochondrial membranes. Total lipids from mitochondrial membranes from SHAM and OVX rats were extracted by the method of Folch et al., saponified and converted to their corresponding fatty acid methyl esters (FAMEs). FAMEs were used to analyze the global fatty acid composition of hippocampal mitochondrial membranes by Gas-liquid chromatography (GLC). Cholesterol (CHOL) content was determined spectrophotometrically in mitochondrial membranes from SHAM and OVX rats. Each column represents the mean ± SEM of (A) CHOL content, (B) relative quantity of each FAME or (C) peroxidizability index (PI) (n=7-8 animals/group). *p<0.05; **p<0.01, Student's t test.

Figure 6. Content, fatty acid composition and peroxidizability index of main phospholipids from hippocampal mitochondrial membranes. Total lipids from mitochondrial membranes from SHAM and OVX rats were extracted and phospholipids were separated by HPTLC. Cardiolipin (CL),

phosphatidylcholine (PC) and phosphatidylethanolamine (PE) were identified by comparison with commercial standards and quantified by densitometric analysis using Image J software. CL, PC and PE spots were scrapped, extracted, converted to their corresponding FAMEs and analyzed by GLC. Each column represents the mean ± SEM of (A) the relative change in each phospholipid content respect to SHAM, (B) relative quantity of each FAME or (C) peroxidizability index (PI) (n=7-8 animals/group). *p<0.05; **p<0.01, Student's t test.

Table 1. Oxygen consumption rates and P/O ratios of freshly isolated hippocampal mitochondria

	SHAM	OVX
NADH-linked respiration (substrate malate-glutamate)		
State 4	22.0 ± 1.0	21.0 ± 2.0
State 3	69.0 ± 3.0	49.0 ± 7.0*
RCR	3.1 ± 0.4	2.6 ± 0.7
State 4_o	43.0 ± 5.0	38.0 ± 5.0
State 3_u	61.0 ± 2.0	63.0 ± 3.0
P/O	2.1 ± 0.3	2.0 ± 0.3
FADH2-linked respiration (substrate succinate)		
State 4	43.0 ± 2.0	43.0 ± 2.0
State 3	68.0 ± 5.0	59.0 ± 6.0
RCR	1.6 ± 0.1	1.4 ± 0.2
State 4_o	49.0 ± 10.0	41.0 ± 12.0
State 3_u	76.0 ± 10.0	54.0 ± 10.0
P/O	1.2 ± 0.1	1.0 ± 0.1

Oxygen uptake rates were evaluated in isolated hippocampal mitochondria from SHAM and OVX rats by high resolution polarography. Resting respiration (state 4) rate was determined with malate-glutamate as complex I substrate or succinate as complex II substrate; active respiration (state 3) rate was determined by adding ADP in both cases. RCR was calculated as state 3/state 4 respiration rates. State 4o was induced by oligomycin (2 µM), while m-CCCP (2 µM) was used to establish state 3u respiration. Oxygen uptake is expressed as ng-at O/min. mg protein. P/O ratios were calculated as ATP production/state 3 O_2 consumption rates. Results are expressed as mean ± SEM (n=3-5 animals/group); *$p<0.05$, Student's t test.

Table 2. Colorimetric assessment of hippocampal mitochondria respiratory chain complex activities

	SHAM	OVX
Complexes I-III (nmol/min. mg protein)	106.0 ± 4.0	103.0 ± 4.0
Complexes II-III (nmol/min. mg protein)	35.8 ± 2.8	33.3 ± 2.2
Complex IV (k´/min. mg protein)	3.1 ± 0.1	3.2 ± 0.2

The enzymatic activity of NADH-cytochrome c reductase (complexes I–III), succinate cytochrome c reductase (complexes II–III) and cytochrome oxidase (complex IV) was evaluated spectrophotometrically in hippocampal mitochondria membranes from SHAM and OVX rats. Results are expressed as mean ± SEM (n=6 animals/group); ns, Student's t test.

Figure 1

A

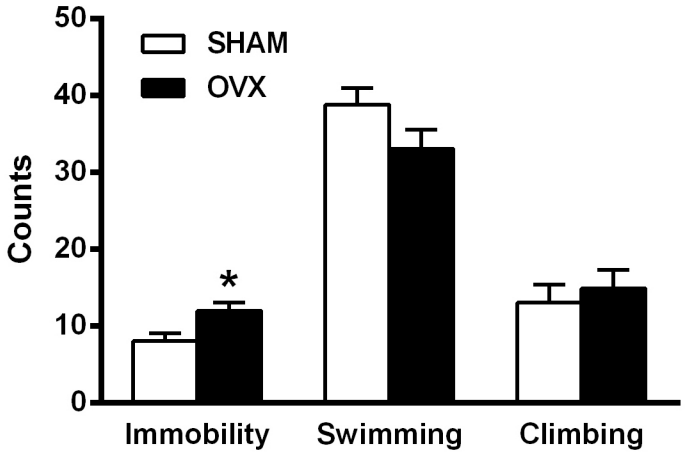
50
40
30
20
10
0
Counts
SHAM
OVX
*
Immobility
Swimming
Climbing

B

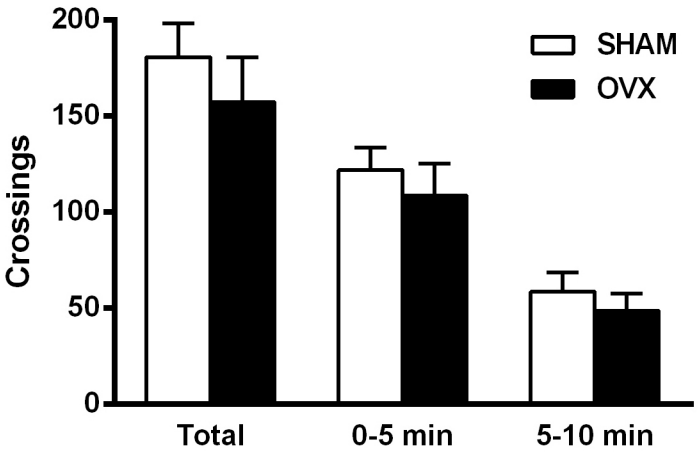
200
150
100
50
0
Crossings
SHAM
OVX
Total
0-5 min
5-10 min

C

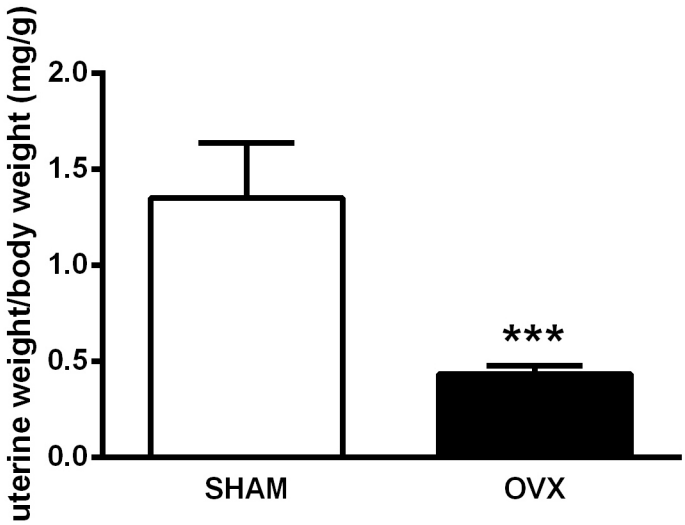
2.0
1.5
1.0
0.5
0.0
uterine weight/body weight (mg/g)
***
SHAM
OVX

Figure 2

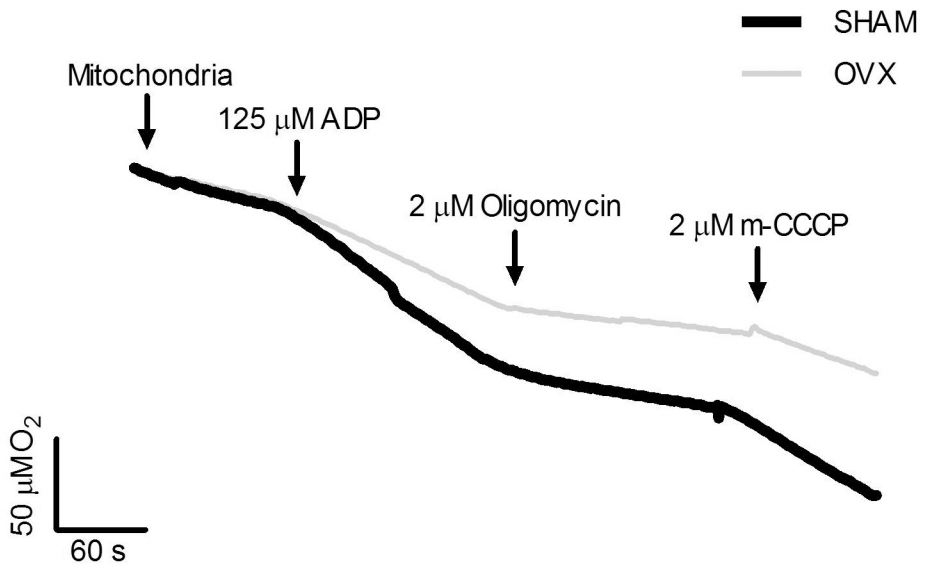
SHAM
OVX
Mitochondria
125 μM ADP
2 μM Oligomycin
2 μM m-CCCP
50 μMO2
60 s

Figure 3

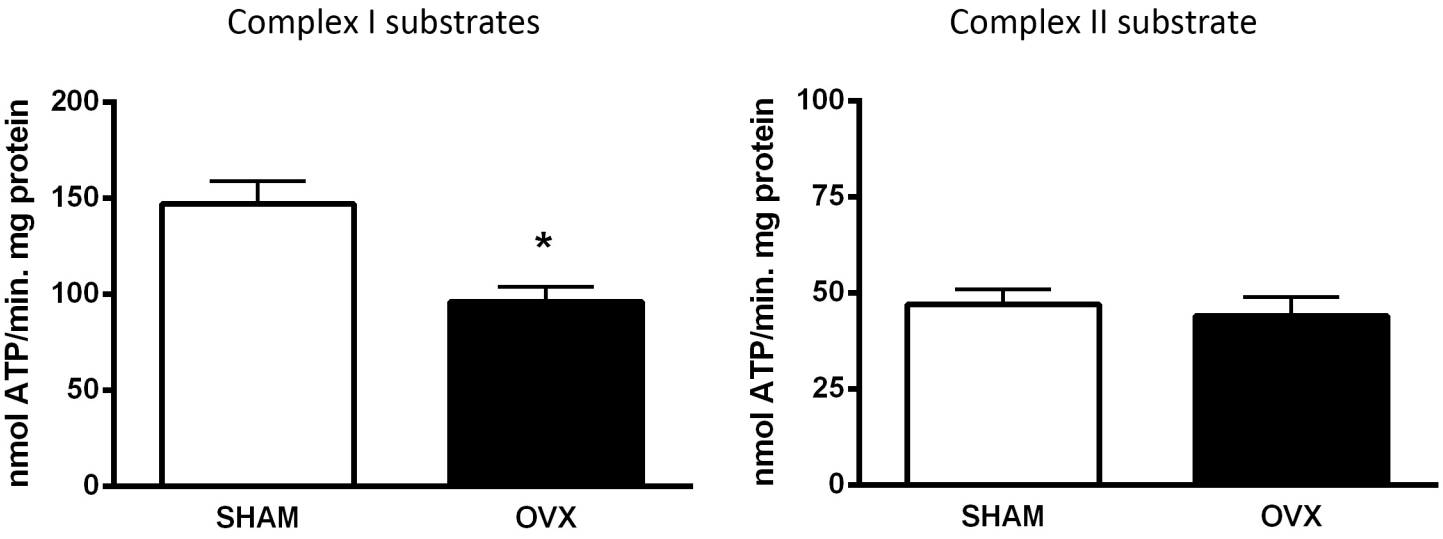
Complex I substrates
nmol ATP/min. mg protein
200
150
100
50
0
*
SHAM
OVX
Complex II substrate
nmol ATP/min. mg protein
100
75
50
25
0
SHAM
OVX

Figure 4

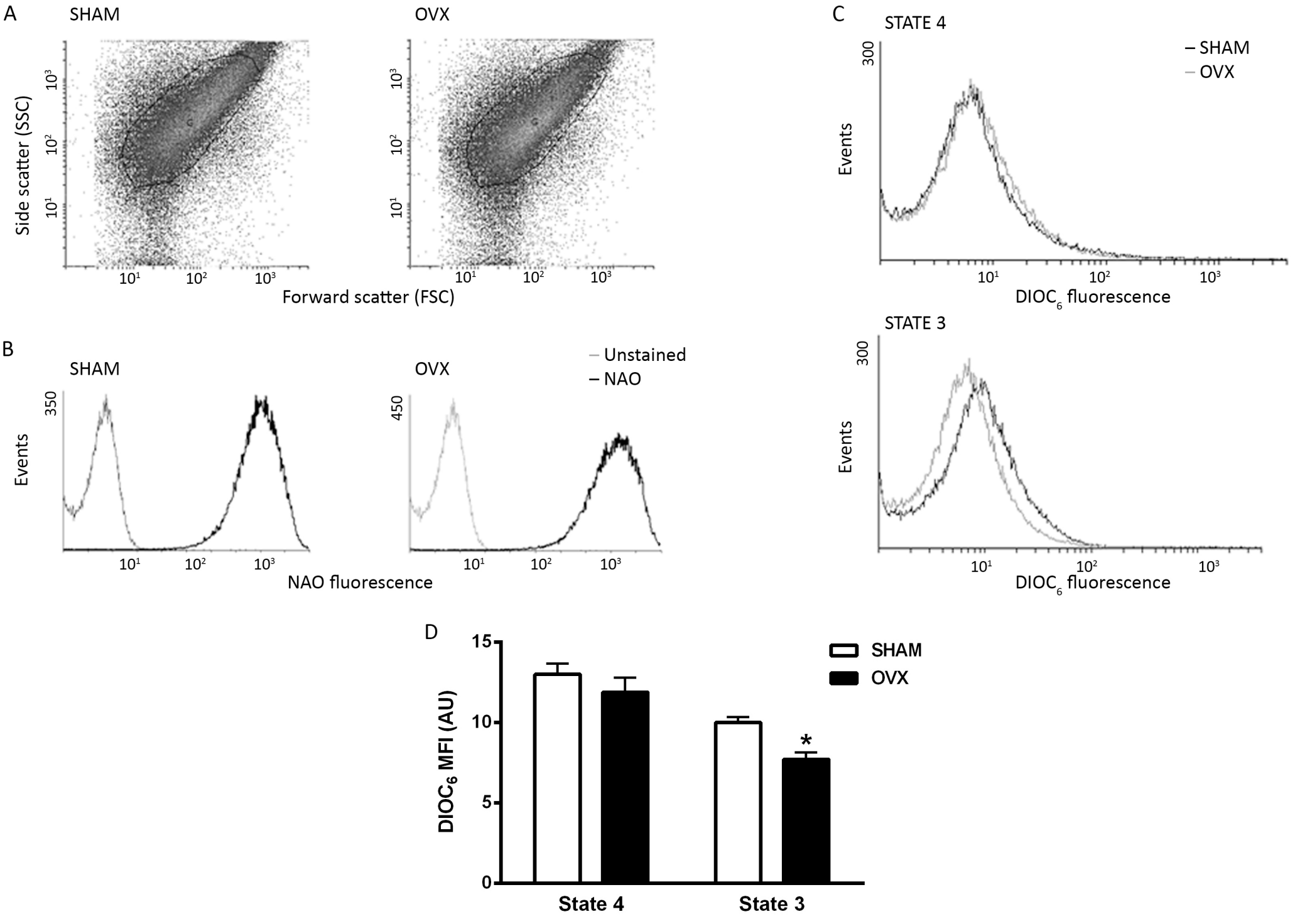
A
SHAM
OVX
Side scatter (SSC)
Forward scatter (FSC)
B
SHAM
OVX
Unstained
NAO
Events
NAO fluorescence
C
STATE 4
SHAM
OVX
Events
DIOC6 fluorescence
STATE 3
Events
DIOC6 fluorescence
D
DIOC6 MFI (AU)
SHAM
OVX
State 4
State 3
*

Figure 5

A

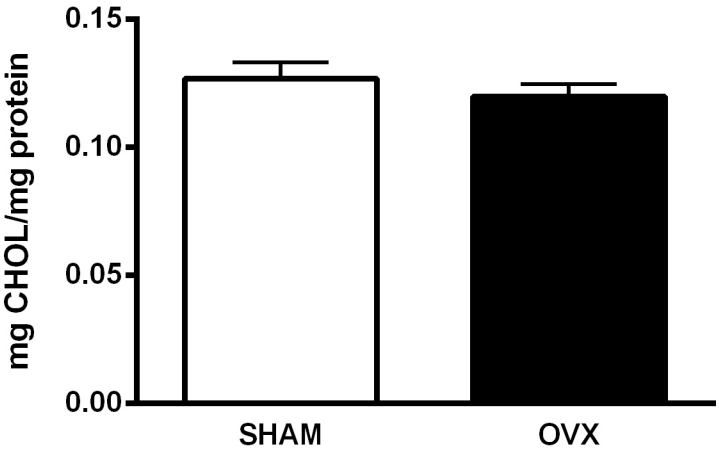
mg CHOL/mg protein
0.15
0.10
0.05
0.00
SHAM
OVX

B

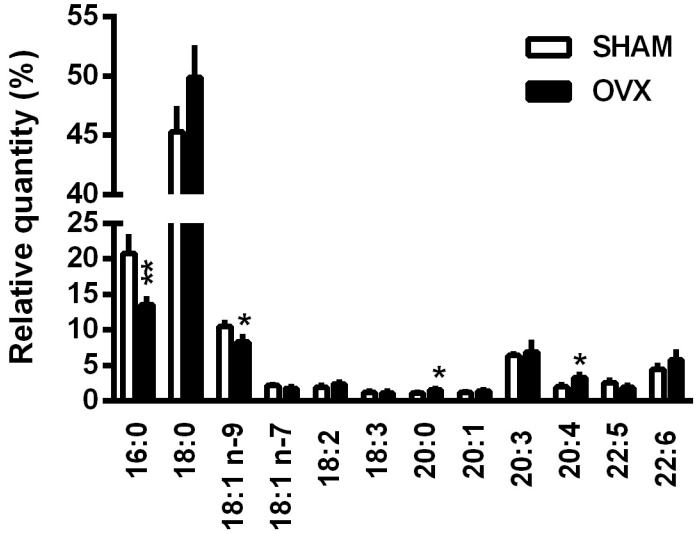
Relative quantity (%)
55
50
45
40
25
20
15
10
5
0
SHAM
OVX
**
*
*
*
16:0
18:0
18:1 n-9
18:1 n-7
18:2
18:3
20:0
20:1
20:3
20:4
22:5
22:6

C

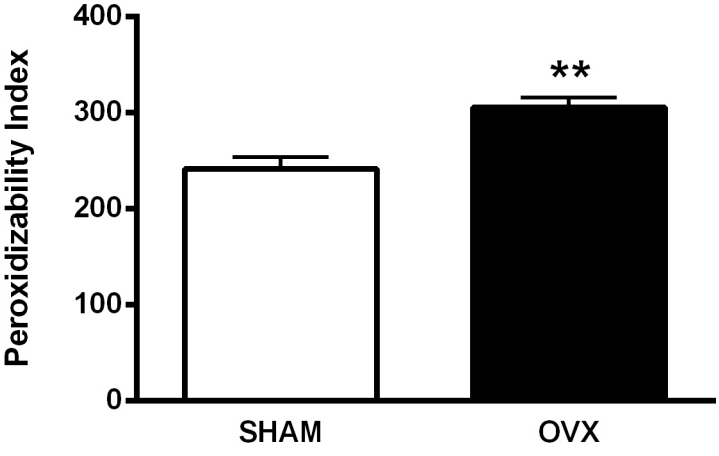
Peroxidizability Index
400
300
200
100
0
**
SHAM
OVX

Figure 6

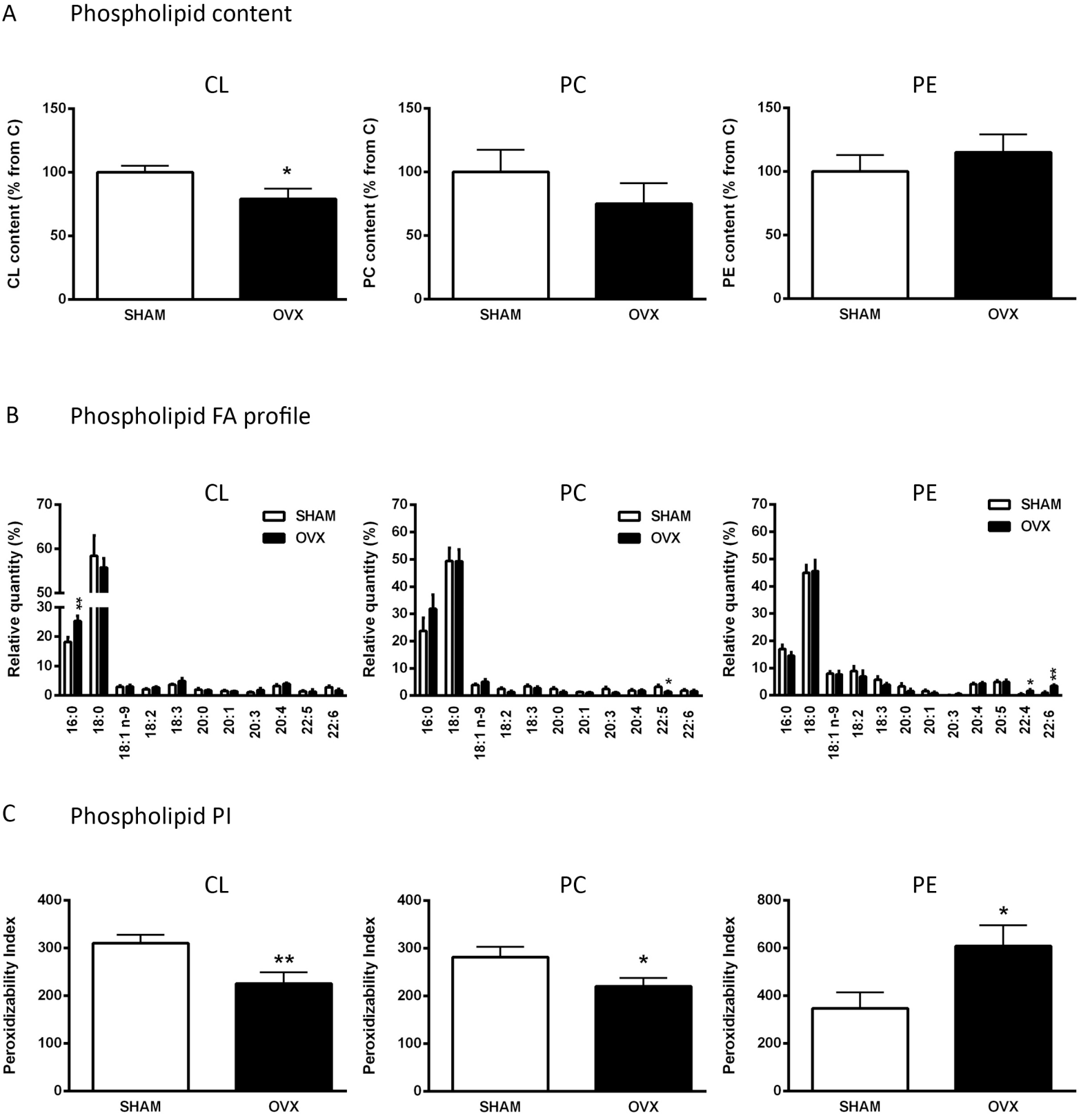
A
Phospholipid content
CL
PC
PE
CL content (% from C)
PC content (% from C)
PE content (% from C)
150
100
50
0
*
SHAM
OVX
B
Phospholipid FA profile
Relative quantity (%)
70
60
50
40
30
20
10
0
**
*
SHAM
OVX
16:0
18:0
18:1 n-9
18:2
18:3
20:0
20:1
20:3
20:4
20:5
22:4
22:5
22:6
C
Phospholipid PI
Peroxidizability Index
400
300
200
100
0
800
600